

Seasonal variations in the station ranging bias and tropospheric zenith delay in SLR

Minkang Cheng (1)

(1) Center for Space Research, University of Texas at Austin, USA (cheng@csr.utexas.edu)

Abstract

Changes in the surface mass loading deform the Earth's surface and cause a modulation of the mass loading center and produce an additional loading potential acting on satellite. A significant seasonal signal in station ranging bias was observed for most tracking stations in the global SLR network. A large part (~60%) of the seasonal ranging bias is due to the surface mass-loading-induced variations in the station position and degree one loading potential affecting on satellite. A part (6%) is due to the high degree surface mass loading induced variation, as well as ~40% due to the errors in modeling of troposphere zenith delay and horizontal gradients. The monthly geocenter solution becomes comparable with the solution from the GPS-based global conversion when the monthly ranging biases were simultaneously estimated for the tracking stations. The effects of the error in the modeling of tropospheric zenith delay and gradients are negligible effects on estimating the geocenter variations and can be separated from ranging bias but cannot be from station height.

Keywords. Geocenter, satellite laser ranging (SLR), origin of ITRF, troposphere zenith delay

1. Introduction.

Geodetic Satellite Laser Ranging (SLR) is an invaluable core technique in numerous geodetic applications. SLR determined C20/C30 become essential component for the GRACE and GRACE-FO science application. The SLR data has provided long-term (over the past four decades), stable determinations of the Terrestrial Reference Frame (TRF) with accurate ties to the center of mass (CM or geocenter) for the entire Earth system, including the solid earth, oceans, cryosphere, surface water and atmosphere. Although high precision for SLR measurement is pursued for all these geodetic SLR applications, however, the systematical error, the well-known "station ranging" and tropospheric biases can affect the realization of ITRF and determination of geocenter variations. Adjusting station ranging bias become standard procedure for all SLR applications. Drożdżewski and Sośnica [2021] conclude that uncalibrated range biases and tropospheric biases can substantially affect the geocenter coordinates, the estimation of tropospheric biases provides more stable station coordinates than the solution with the estimation of range biases. However, a significant fluctuation was observed in the estimated ranging bias, such as for station 7941 (MLRO) (Fig. 2 of Luceri et al., 2019). It is required to improve our understanding of the nature of the seasonal signal in the station ranging bias and its effect on the realization of ITRF and the origin of ITRF. Following the procedure described by Cheng et al. [2013], a time series of monthly solutions was determined from the SLR data over a calendar month from 5 geodetic satellites, including Starlette, Ajisai, Stella, LAGEOS 1 and 2. The solution parameters include the satellite state vector (3-day arc) and other dynamical parameters, including 12-hour C_D or C_T , the lower portion of the gravity field up to degree 5, three components of the geocenter motion, \vec{r}_{cm} .

This approach provides a unified recovery of the gravity signals from SLR data [Cheng and Ries, 2022]. The monthly station ranging bias or tropospheric zenith delay and horizontal gradients are also estimated for those tracking stations withing each calendar month to study the seasonal variation in ranging bias, tropospheric zenith delay and horizontal gradients in different cases.

This paper reviews the measurement models of SLR data (and the tropospheric zenith delay) in section 2, the estimated ranging bias either globally or monthly from multi-satellite SLR data will be also presented in section 2, and the estimated tropospheric zenith delay and gradients in section 3, the high degree loading induced the station displacement will be discussed in section 4. The effects of station height and the ranging bias on estimation of geocenter variation in section 5. A summary is given in Section 6.

2. SLR ranging bias

The Satellite Laser Ranging (SLR) system measures the two-way Time-of-Flight (TOF) between a pulse emitted from the laser transmitter at the ground station and the reception of the pulse returned from the onboard Laser Retro-reflector Array (LRA) on the orbiting satellite. The TOF multiplied by the speed of light gives the round-trip distance in meters. The time interval counter records the two-way distance with cm-level precision. The one-way range is computed as

$$\rho_{1way} = \frac{\rho_{2way}}{2} + \Delta a_i - \Delta CoM + R_b + \Delta GR + \Delta \epsilon \quad (1)$$

where $\Delta \epsilon$ is the unknown random error. Several corrections are applied, including (1) the atmosphere correction Δa_i including the tropospheric wet/dry delay, (2) the center of mass offset (ΔCoM) between the LRA and the satellite center of mass, (3) the relativistic light-time correction (ΔGR), and (4) a station dependent range bias (R_b) if known or estimated. A time bias may also be applied to the observation time tag.

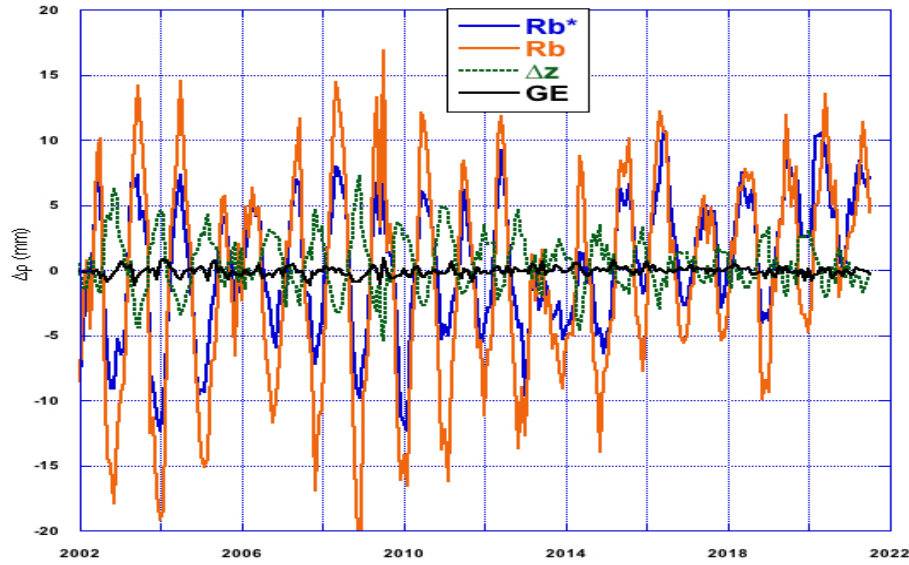
The laser range residuals $\Delta \rho$ after orbit fitting can be expressed as $\Delta \rho = R_b + T_b d\rho / dt + \epsilon$. The apparent range bias (R_b), time bias (T_b), and a polynomial ϵ were adjusted in a path-by-path least-squares fit to the residuals for data editing and precision evaluation. The averaged station path range bias R_b was found to be a few mm to 1 cm or more from the analysis of the residual time series for Lageos-1 over the period from January 2002 to December 2020. The time series of the path range bias often appears to be varying with a small seasonal signal, which was hidden by the high-frequency fluctuations for most stations. In this study, the monthly station ranging bias (for those tracking stations over each calendar month) was adjusted along with the geocenter coordinates in solution over the period from January 2002 to December 2020.

2.1 Seasonal variations in ranging bias.

A significant seasonal signature appears for most stations. For example, the annual amplitude is estimated to be 5.01 mm for 7090, 4.6 mm for 7941 and the largest amplitude of 9.7 mm for 7249. Figure 1 shows the monthly estimate of the ranging bias for station 7090 from 5 satellites (Starlette, Ajisai, Stella, LAGEOS-1 and LAGEOS-2). A linear trend is visible for

most of the stations with the largest rate of ~ 2.8 mm/year. This indicates that possible seasonal loading signals have been captured and retained in the SLR data during the laser pulse traveling. The estimated seasonal range bias could also be contributed from (1) the error in the modeling of tropospheric zenith delay and gradients, (2) the high-degree surface mass loading, and (3) additional degree one loading potential affecting on satellite. Those effects are discussed follows.

Figure 1 Monthly estimate of the laser ranging bias (R_b^* and R_b) and correction of troposphere delay (Δz) for Station 7090, where R_b^* is obtained from estimating range bias only, while R_b is obtained from simultaneously estimating the range bias, troposphere delay (Δz) and horizontal gradients (G_e)



3. Tropospheric zenith delay and horizontal gradients

A part of the estimated station ranging bias may be due to deficiencies in the model for the atmosphere delay in response to the seasonal variations in temperature and pressure of the tracking stations. The total tropospheric zenith delay can be modeled (similar to the model for VLBI) based on 2010 IERS conversion [Eq. 9.12, Petit and Luzum, 2010] as

$$DL = (zd + \Delta z)M_{mpf}(z) + m_g(e)(G_N \cos(A) + G_E \sin(A)) \quad (2)$$

where the zd is the total tropospheric zenith delay from the model of Mendes and Pavlis [2004]. The $M_{mpf}(z)$ is the mapping function from Mendes and Pavlis [2002]. The G_N and G_E are the North and East component of the horizontal gradients in the atmosphere for the azimuth A , $m_g(e)$ is the mapping function of Chen and Herring [1997]. The model for the horizontal gradients is not available yet at present in processing SLR data.

In this study, the Δz , G_N and G_E for the atmosphere horizontal gradients are simultaneously

adjusted with the station ranging bias and the geocenter coordinates in solution. Figure 1 shows the seasonal signals appearing in the time series of the estimated ranging bias, Δz and horizontal gradients for the station 7090. Table 1 compares the annual amplitude and phase for 7090 from solution of the 5 cases: 1) estimate R_b only, 2) simultaneously estimate R_b , Δz and hg (horizontal gradients, G_N and G_E), 3) estimate only Δz and hg only, 4) estimate Δz , hg and the station height (U_p) with 1.5 cm constraint applied.

Table 1 - Seasonal amplitude (A:mm) and phase (ψ : degree) for the error in the zenith delay (Δz), and the horizontal gradients (hg: G_N and G_E), along with estimating range bias (R_b), or the station height (U_p) for station 7090.

Case	Solution	R_b (A/ ψ)	Δz (A/ ψ)	G_N (A/ ψ)	G_E (A/ ψ)	ΔU_p (A/ ψ)
1	R_b only	5.01/154				
2	$R_b + \Delta z + hg$	8.56/152	2.05/327	0.07/261	0.16/69	
3	$\Delta z + hg$		1.61/148	0.22/187	0.34/18	
4	$U_p + \Delta z + hg$		0.26/238	0.05/345	0.15/19	7.36/332

Results in Table 1 show that the annual signal in R_b from Case 1 (as total effects of R_b , and errors in the modeling of troposphere delay and the horizontal gradients) is smaller than R_b from the case 2 by 41% because the phase offset of ~ 180 degrees results in cancelation between R_b and troposphere delay (Δz). The effect of the horizontal gradients is rather small as shown in Figure 1. It is only $\sim 2\%$ of R_b (8.56 mm), but the amplitude of R_b will be increased by 9% if the effects of hg (G_N and G_E) were not adjusted. However, the Δz is $\sim 24\%$ of the R_b (8.56 mm), but the amplitude of R_b is significantly reduced from 8.56 mm to 4.43 mm if Δz was not adjusted because of the cancelation with the Δz . Thus, $\sim 60\%$ of the estimated ranging bias (8.56 mm) in Case 2 may from the surface loading change. Comparing the results from different combinations of estimates, the troposphere delay (Δz) and horizontal gradients (hg) can be separated from simultaneously estimating with the loading induced range bias from SLR data as shown in Case 2 in Table 1. The Δz and hg in Case 4 in Table 1 are estimated along with adjusting station height (U_p) with a 1.5 cm constraint applied. The values for U_p , Δz and hg will be changed depending on the constraint applied for the station height estimate. In any case, Δz cannot be separated from the surface loading induced change in the station height. Thus, the estimated station height from SLR data or the ITRF2020 solution may contain the signals from the errors in the modeling of troposphere delay and the horizontal gradients. An improved model for the troposphere delay and horizontal gradients is required.

The horizontal gradients are not part of the standard SLR analysis yet, but the hydrostatic (and wet) north and east gradient components ($G_{n,h}$, $G_{e,h}$, $G_{n,w}$ and $G_{e,w}$) become operational products in VMF30 (the Vienna Mapping Functions 3 for optical frequencies). The VMF30 model comprises the zenith delays and mapping functions, as well as linear horizontal gradients. The mapping function coefficient in terms of a mean value, the annual and semi-annual terms are derived from ray-traced delays generated by an in-house ray-tracing software [Janian et al, 2020]. Unfortunately, the VMF30 mapping function (vmf3o.f90) is not suitable for SLR data processing [personal communication with Janian,

2023]. The amplitude of annual variations in the hydrostatic component for station 7090 is estimated to be 0.105 mm for $G_{n,h}$ (north) and 0.011 mm for $G_{e,h}$ (east) from the VMF3O model. The annual amplitudes for wet components are ~ 0.002 mm. In comparing with the results for G_N and G_E in Table 1, SLR estimate could provide a constraint on the VMF3O model.

4. High degree surface loading induced in the station displacement.

The surface density changes (or anomalies) will result in a three-dimensional displacement of a station represented by the vector $\vec{s}(\phi, \lambda)$ based on Farrell's [1972] loading theory. Based on Eq. (9) of Trupin et al, (1992) and Wahr et al. (1998), the high degree loading induced global distribution of the annual variations of the surface deformations can be calculated from the time series of GRACE monthly solutions with size of 60x60 and 300 km smoothing. It can be shown that the largest scale annual variation occurs over the Amazon, Himalayan, Africa, Greenland and Russia. The maximum amplitude is estimated to be $\sim 18, 3, 2$ mm for the vertical displacement s_r , and the horizontal displacement s_ϕ and s_λ , respectively. Table 2 shows the annual amplitude (for 7090) of the displacement in ENU (local East, North, and vertical Up) coordinates computed from the CSR GRACE monthly solutions over the period from August 2002 to August 2016. The results are compared with the seasonal variations estimated in the ITRF2020 solution (Atamimi, et al, 2022), as well as the changes in station height estimated along with the geocenter parameters (X, Y and Z) from SLR data of 5-satellite over the time period from Jan 2002 to Dec 2021.

The seasonal signal measured by GRACE is expected to represent the true load effects of high degree (> 1) on the stations. However, the seasonal signals from the ITRF2020 solution represent the total (degree one to higher degree and order) loading effects on stations. The amplitude and phase in the height from SLR data (as shown in Table 2) were estimated with a 1 mm constraint, but will be 8.05 mm and 337 degrees with a constraint of a 1.5 cm. Denote A^e as the annual amplitude in the height (Up) estimated from SLR, A^G is that from the higher degree loading measured by GRACE. On average, the ratio of A^e/A^G is estimated to be 0.29 for 46 SLR data sites with 1.5 cm constraints applied. The ratio can be reduced to 0.19 with 10 cm constraints applied. Thus, additional information is required to justify whether the applied constraint is appropriate for accounting for the high degree loading effects in the approach by estimating the geocenter variation along with station height for the global SLR tracking network.

Table 2 - Comparison of Annual variation in ENU from GRACE, TRF2020 and SLR

Solution	E(mm/deg)	N(mm/deg)	Up(mm/deg)
GRACE	0.228/322	0.156/299	1.77/327
TRF2020	0.851(+0.24)/64(± 46)	2.69(± 0.44)/269(± 46)	3.65(± 0.31)/317(± 45)
This study			3.61(± 0.1)/315(± 5)

If $\Delta r = \sqrt{\Delta x^2 + \Delta y^2 + \Delta z^2}$ represents the variation along the radial direction, the annual amplitude in radial is estimated to be 0.47 mm for 7090 from the higher degree loading induced seasonal signals measured by GRACE. In average, the ratio of $\Delta r/R_b$ is estimated to be ~ 0.06 for the annual amplitude in radial with respect to the estimated ranging bias (8.05 mm) from SLR data. This ratio might suggest that the effects of the higher degree loading induced variations could only be $\sim 6\%$ of the estimated station ranging bias assuming $\Delta \rho^l \approx \bar{\rho} \cdot \Delta \bar{R}_s / \rho \approx \Delta r$.

5. Effects on determination of geocenter variation.

Monthly geocenter variation can be obtained by adjusting the troposphere delay, the horizontal gradients, and station height in different cases. The annual amplitude and phase (ψ) of geocenter variations estimated along with R_b , Δz and hg (as shown for Case 2 in Table 1) are estimated to be $1.8 \pm 0.2 / 46 \pm 4$ for X, $2.7 \pm 0.2 / 303 \pm 4$ for Y and $2.4 \pm 0.3 / 27 \pm 4$ for Z component. Those solution is comparable with the solution from the global inversion based on the GPS/OBP/GRACE (Wu et al., 2012), and the TN13 (JPL time series, GRACE Technical Note 13, Felix, 2020). The solution can be considered as a better estimate of geocenter motion from SLR data when all errors in R_b , Δz and hg (G_N and G_E) are removed. Effects of Δz and hg (G_N and G_E) (corresponding to Case 3 in Table 1) are negligible on the estimate of the geocenter variations because the atmosphere delay in SLR data is not related to the surface-mass loading-induced site variations. Thus, the seasonal signal appearing in station ranging biases and the tropospheric delay must be considered in order to precisely characterize the loading mass center shift. However, the solution of the geocenter parameters estimated along with the station height is highly dependent on the constraint applied.

The ranging bias can be expressed as $\Delta R_b = (\Delta \bar{\rho} \cdot \bar{R}_s + \bar{\rho} \cdot \Delta \bar{R}) / \rho \approx \Delta \rho_b^s + \Delta \rho_b^l$. While the $\Delta \rho_b^l$ could only be $\sim 6\%$ in the estimated station ranging bias as discussed in Section 4. Thus, part of the seasonal signal in the R_b could be due to the degree one loading potential acting on the satellite orbit represented by $\Delta \rho_b^s$. Further analysis for the degree one perturbation on satellite orbit is required.

6. Summary

We show that the satellite laser ranging measurement has captured a significant seasonal signal with the annual amplitude of a few mm during the laser light pulse traveling. Part ($\sim 40\%$) of this signal is contributed from the mismodeling of the troposphere delay (Δz) and without modeling the atmospheric horizontal gradients (hg) in SLR data processing. The Δz and hg can be separated from the surface mass loading induced ranging bias, and less affect the estimating of the geocenter variation from SLR data. A large part ($\sim 60\%$) of the observed seasonal signal appearing as ranging bias is the effects of the surface loading induced displacement of the tracking site and the additional potential acting on satellite orbit during the laser pulses traveling.

Acknowledgments. This research was supported by NASA grants 80NSSC20K0766. The author thanks ILRS for providing the satellite laser ranging data to the geodetic satellites, and

John Ries at CSR supported the analysis through maintaining the SLR network setup and editing the SLR data. We thank the Texas Advanced Computing Center for providing computational resources.

References

- Chen, G., and T. A. Herring, Effects of atmospheric azimuthal asymmetry on the analysis of space geodetic data, *J. Geophys. Res.*,102(B9), 20,489–20,502, <https://doi.org/10.1029/97JB01739>, 1997.
- Cheng, M. K., J. C. Ries, B. D. Tapley, Geocenter Variations from Analysis of SLR data, in Reference Frames for Applications in Geosciences, IAG (International Association of Geodesy) Symposia, Vol. 138, 19-26, Springer, 2013.
- Cheng, M. K., J. C. Ries, C_{20} and C_{30} Variations from SLR for GRACE/GRACE-FO Science Applications, *JGR*, Doi: 10.1029/2022JB025459, 2022.
- Drozdowski, M., and K. Sosnica, Tropospheric and range biases in Satellite Laser Ranging, *J. Geodesy*, 95:100, <https://doi.org/10.1007/s00190-021-01554-0>, 2021.
- Farrell, W. E., Deformation of the Earth by surface loading, *Rev. Geophys.*, 10, 761-797, 1972.
- Janina Boisits, Daniel Landskron, Johannes Böhm, VMF3o: the Vienna Mapping Functions for optical frequencies, *Journal of Geodesy*, 94:57, <https://doi.org/10.1007/s00190-020-01385-5>, 2020.
- Luceri, V., M. Pirri, J. Rodríguez, G. Appleby, E. C. Pavlis, H. Müller, Systematic errors in SLR data and their impact on the ILRS products, *Journal of Geodesy*, 93:2357–2366, <https://doi.org/10.1007/s00190-019-01319-w>, 2019.
- Mendes, V. B., Prates, G., Pavlis, E. C., Pavlis, D. E., and Langley, R. B., Improved mapping functions for atmospheric refraction correction in SLR, *Geophys. Res. Lett.*, 29(10), 1414, doi: 10.1029/2001GL014394, 2002.
- Mendes, V. B., and Pavlis, E. C., High-accuracy zenith delay prediction at optical wavelengths," *Geophys. Res. Lett.*, 31, L14602, doi: 10.1029/2004GL020308, 2004.
- Petit, G. and B. Luzum, IERS Conventions, IERS Technical Note No. 36, International Earth Rotation and Reference Systems Service. Frankfurt, Germany, 2010.
- Trupin, A., S., M. F. Meier, J. Wahr, Effects of melting glaciers on the Earth's rotation and gravitational field: 1965-1984, *Geophys. J. Int.* 108, 1-15, 1992.
- Wahr J., M. Molenaar, F. Bryan, Time variability of the Earth's gravity field: Hydrological and oceanic effects and their possible detection using GRACE, *J. Geophys. Res.*, 103 B12, 30,205-30,229, 1998.
- Wu, X., J. Ray and T. van Dam, Geocenter motion and its geodetic and geophysical implications, *J. Geodyn.*, 58, 44-61, <https://doi.org/10.1016/j.jog.2012.01.007>, 2012.